Check for updates

Conversion of levulinic acid to γ-valerolactone over Ru/Al₂O₃–TiO₂ catalyst under mild conditions

Ruifeng Wang,[ab] Lungang Chen,[b] Xinghua Zhang, [ID] *[b] Qi Zhang, [ID] [b] Yuping Li,[b] Chenguang Wang[b] and Longlong Ma[b]

Novel catalytic material with high catalytic activity and hydrothermal stability plays a key role in the efficient conversion of levulinic acid (LA) to γ-valerolactone (GVL) in water. In this study, mixed oxides Al₂O₃–TiO₂, Al₂O₃–MoO₃ and Al₂O₃–Co₃O₄ were synthesized by co-precipitation using aqueous solution of NaOH as precipitant. Ru catalysts supported on mixed oxides were prepared by impregnation method and their catalytic performances were tested in the hydrogenation of LA to GVL on a fixed bed reactor. The physicochemical properties of the catalysts were characterized by XRD, H₂-TPR, NH₃-TPD, and BET techniques. The TiO₂ component significantly affected the acidity of the catalyst, and thus its catalytic activity for the GVL yield was affected. The desired product GVL with a yield of about 97% was obtained over the Ru/Al₂O₃–TiO₂ catalyst under mild conditions (WHSV = 1.8 h⁻¹, T = 80 °C). Moreover, the catalyst Ru/Al₂O₃–TiO₂ exhibited excellent thermal stability in the test period of time.

Introduction

γ-Valerolactone (GVL), a versatile platform compound with high stability and low toxicity, can be used as fuel and viable intermediate for production of chemicals and solvents.[1,2] It had been proposed to be one of the top 12 platform chemicals by the US Department of Energy.[3] Moreover, GVL has been perceived as a potential replacement for ethanol in gasoline–ethanol blends because of their better lubricity, higher boiling points and low solubility in water.[4] GVL can be produced from levulinic acid (LA) by hydrogenation and subsequent cyclization,[5] and LA can be directly produced from lignocellulosic biomass via a simple hydrolysis process with pristine protonic acids.[6,7] Therefore, it is an attractive route to produce GVL from LA economically.

In the past years, extensive research had been conducted on the catalytic conversion of LA to GVL.[5,8] Selective hydrogenation of LA to GVL was found to be an efficient method. Typically, base metal catalysts, such as Cu, Ni and Co, often show lower catalytic activity and relatively high temperature is required.[9] To improve the catalytic activity, base metal catalysts modified by noble metal were explored. Results demonstrated that hydrogenation of LA to GVL can be achieved over the bi-metallic catalysts supported on neutral supports like active carbon, TiO₂, ZrO₂ and acid support like γ-Al₂O₃ at the temperature of 180–250 °C.[10–13] It can be seen that high temperature is required

aNano Science and Technology Institute, University of Science and Technology of China, Suzhou 215123, P. R. China

bGuangzhou Institute of Energy Conversion, Chinese Academy of Sciences, Guangzhou 510640, P.R. China. E-mail: zhangxh@ms.giec.ac.cn; Fax: +86 20 8705 7789; Tel: +86 20 8705 7790

in the conversion of LA to GVL over the base metal catalyst, which inevitably incur an energy cost for viable applications.

Fortunately, the conversion of LA to GVL can also be catalysed efficiently by noble metal catalysts under mild condition because of their excellent catalytic activity for hydrogenation.[14–16] It had been reported that GVL yields are more than 90% over the catalysts of Ru, Pt and Pd at 90 °C.[17,18] Sudhakar *et al.*[19] had reported that hydroxyapatite (HAP)-supported Ru catalyst exhibited 99% yield of GVL from LA by hydrogenation at 70 °C and 0.5 MPa H₂ pressure. However, LA conversion decreased to below 90% when the Ru/HAP was repeatedly used for 5 times. It is found that about 47% of Ru were leached into solution when Ru/Al₂O₃ was used as catalyst in the conversion of LA to GVL.[18] Deteriorated hydrothermal stability of the catalyst has become a bottleneck restricting the production of GVL from LA. To improve the hydrothermal stability of catalyst, hydrogenation catalysts supported on water-tolerant materials, such as carbon[20] and silica,[21] had been tested. However, these catalysts had a low yield and selectivity for GVL. Chia *et al.*[22] developed a new conversion method for the production of GVL from alkyl levulinates over ZrO₂ catalysts. Rapid deactivation of the catalyst was also observed during a 100 h period. Arguably, more studies are required to develop a novel catalyst with longer service life.

The mixed oxides are usually attractive for the improvement of catalytic performance.[23] To develop a novel material with high catalytic activity and hydrothermal stability, mixed oxides Al₂O₃–TiO₂, Al₂O₃–Co₃O₄ and Al₂O₃–MoO₃ were prepared in this study, and were used as carrier for Ru-based catalyst. Also, the catalytic activity was tested in the conversion of LA to GVL in water. It was found that Ru/Al₂O₃–TiO₂ catalyst is capable of the efficient synthesis of GVL from LA in a continuous fixed bed

reactor under mild condition. TiO$_2$ is pristine material with excellent hydrothermal stability.[23] The screening investigations have indicated that Ru/TiO$_2$ catalyst can offer catalytic activity in the conversion of LA to GVL.[24] For comparison purposes, the pure oxide TiO$_2$ and Al$_2$O$_3$ were also used as carrier for Ru-based catalyst and were tested in the conversion of LA to GVL.

Experimental

Materials and catalyst preparation

Mixed oxides Al$_2$O$_3$–TiO$_2$, Al$_2$O$_3$–Co$_3$O$_4$ and Al$_2$O$_3$–MoO$_3$ were prepared based on the following methods.

Al$_2$O$_3$–MoO$_3$: solutions of (NH$_4$)$_6$Mo$_7$O$_{24}$ and Al (NO$_3$)$_3$ were mixed. With continuous stirring, sodium hydroxide solution was added into the mixed solution at 70 °C until the pH of the solution reached an approximate value of 8. The obtained precipitate was filtered and washed with distilled water. Then the obtained solid was dried at 80 °C for 12 h and calcined at 500 °C for 5 h, by which the complex oxide Al$_2$O$_3$–MoO$_3$ (mole ratio of Al : Mo = 1 : 1) was prepared and was designated as Al–Mo.

Similar to that of Al$_2$O$_3$–MoO$_3$, complex oxide Al$_2$O$_3$–Co$_3$O$_4$ (mole ratio of Al : Co = 1 : 1) was prepared using Al(NO$_3$)$_3$·9H$_2$O and Co(NO$_3$)$_2$·6H$_2$O as precursor and designated as Al–Co. Al$_2$O$_3$–TiO$_2$ (mole ratio of Al : Ti = 1 : 1) was prepared using TiCl$_4$ and Al(NO$_3$)$_3$ as precursor and designated as Al–Ti.

Ru-based catalysts with 5 wt% Ru loadings were prepared by impregnation. Specifically, support was dipped into the RuCl$_3$ solution (0.1 mol l^{-1}), followed by treating with ultrasonic irradiation for 2 h. After impregnation for 12 h, the solution was evaporated to dryness. Then, the obtained solid was dried at 120 °C overnight and calcined at 550 °C for 4 h. For comparison, Ru catalysts supported on Al$_2$O$_3$ and TiO$_2$ were also prepared and designated as Ru/Al, Ru/Ti, respectively.

The prepared catalysts were crushed, sieved through 0.83–0.38 mm mesh before use.

Chemicals used in this study are C.P. reagents and purchased from Aladdin's Reagent Company.

Catalyst characterization

Specific surface area (S_{BET}), pore diameter and pore volume of catalysts were determined by N$_2$ isothermal adsorption (77 K) on physical adsorption instrument (Quantachrome Corporation NOVA-2100) according to BET and BJH theoretical models. The catalyst was pretreated at 200 °C for 12 h under vacuum condition before N$_2$ adsorption.

The crystal structure of the catalysts were analyzed by X-ray diffraction radiation (X Per Pro MPD with Cu Kα (λ = 0.15406 nm) radiation, Philip). The transmission electron microscope (TEM) images of the catalysts were obtained on an instrument (JEM-2100F).

The H$_2$-TPR (H$_2$ temperature-programmed reduction) analysis of catalyst was conducted on a chemisorption apparatus. The catalyst samples (100 mg) were pretreated at 300 °C for 1 h under an Ar flow and subsequently cooled to 50 °C. The reduction temperature increased to 800 °C with 10 °C min^{-1} in

the flow of reduction gas (H$_2$ + N$_2$, 40 ml min^{-1}). The H$_2$ consumption was monitored by a thermal conductivity detector (TCD).

The XPS (X-ray photoelectron spectroscopy) analysis of Ru catalyst was carried out on the instrument of Thermo Scientific ESCALAB 250Xi employing a monochromated AlKα X-ray source.

The NH$_3$-TPD (NH$_3$ temperature-programmed desorption) analysis was also conducted on a chemisorption apparatus equipped with a TCD detector. Before ammonia adsorption, the catalyst samples (100 mg) were *in situ* reduced for 2 h at 300 °C in the flow of hydrogen and purged at 100 °C for 1 h with helium. The detailed method was described in a literature.[25] The catalyst was pretreated at 200 °C under vacuum (1 × 10^{-4} Pa) for 1 h. Pyridine was introduced in the IR cell at room temperature. Desorption was carried out at 200 °C, and the catalyst was evacuated for 10 min prior to recording the IR spectra.

Experimental procedure

The catalytic activity test was performed in a fixed-bed stainless steel tube reactor (10 mm internal diameter). This reaction system is equipped with a mass flow controller for H$_2$ supply and a HPLC pump for the continuous injection of levulinic acid solution. The pelletized catalyst (2.0 g) was packed in the middle of the reaction tube. The catalyst was reduced in the flow of H$_2$ (40 ml min^{-1}) for 4 h at 360 °C. Then, the hydrogenation reaction was conducted at desired temperature. The feedstocks were the mixtures of 95 wt% H$_2$O and 5 wt% LA. Liquid product collected every 10 h was analyzed off-line by GC (SHIMADZU GC2014 with a flame ionization detector and a column of HP (30 m × 0.25 mm × 0.25 μm)) using external standard method. The vaporization temperature was 250 °C, and the oven temperature program ranged from 50 to 250 °C at the rate of 10 °C min^{-1}. LA conversion (X_{LA}) and product yield (Y_P) were calculated based on the following formulas:

$$X_{LA} = 100\% - \frac{\text{mol of reactants after reaction}}{\text{mol of reactants in feedstock}} \times 100\% \quad (1)$$

$$Y_P = \frac{\text{mol of each product}}{\text{mol of reactants in feedstock}} \times 100\%. \quad (2)$$

The gas product obtained from the hydrogenation process was analyzed on a Gas Chromatogram (Agilent 6980) with a TCD (Thermal Conductivity Detector) and a FID (Flame Ionization Detector) using the external standard method.

The concentration of Al and Ru ions remaining in the liquid samples was determined by ICP-AES (Inductively coupled plasma-atomic emission spectroscopy, IRIS Advantage 1000, Thermo Electron Corporation).

Results and discussion

Catalyst characterization

The textural properties of Ru catalysts, supported on different oxides, were summarized in Table 1 and Fig. 1. The pore size

Table 1 Porous structure characterization of the different catalysts

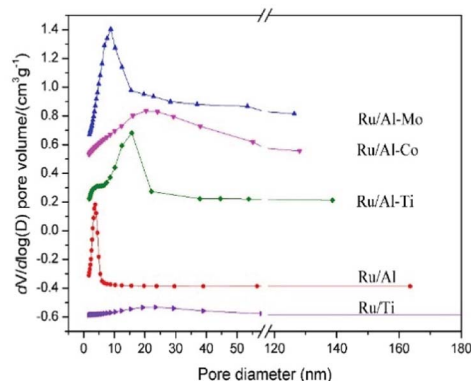| Catalyst	S_{BET} (m^2 g^{-1})	Pore volume (cm^3 g^{-1})	Pore size (nm)
Ru/Al–Mo	243	0.65	10.7
Ru/Al–Co	77	0.27	14
Ru/Al–Ti	98	0.24	9.8
Ru/Al	176	0.18	4.1
Ru/Ti	11	0.04	14.5

Fig. 1 Pore size distribution of different Ru catalysts.

distribution of Ru catalysts supported on different mixed oxides is in the range of 2–50 nm. Compared with Ru/Al catalyst, the most probable pore diameter of the Ru catalysts supported on mixed oxides become larger. It should be noted that the surface areas and pore volumes of Ru/Al–Mo are larger than that of Ru/Al catalyst. A possible reason is that a large part of Al$_2$O$_3$ is dispersed on the surface of MoO$_3$, resulting in the increase of the surface areas and pore volumes.

XRD patterns of samples were gathered in Fig. 2. The peaks assigned to Ru were not significant for all samples. Only one weak diffraction peak positioned at the 2θ of 38.4° was observed for all fresh catalysts, which were assigned to the (1 0 0) plane of Ru. This result suggests good dispersion of Ru metal. The size of Ru particles supported on different mixed oxides was determined by TEM. As shown in Fig. 3, most of Ru particle are in the range of approximately 2–5 nm. Especially for Ru/Al–Ti catalyst,
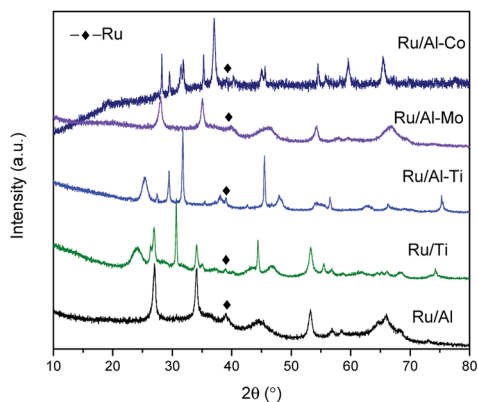

Fig. 2 XRD patterns of different Ru-based catalysts.

the particle size of Ru are all in the range of 1–3 nm and the average particle size is 1.76 nm. Primo et al.[24] had reported that the Ru particle with the size of about 2 nm exhibited the highest catalytic activity for hydrogenation.

Fig. 4 gathered the H$_2$-TPR profiles of the Ru-based catalysts. The peaks, positioned in the range of 90–250 °C, were observed for all of catalysts, which are attributed to the reduction of RuO$_2$. The effect of support on the reduction of active metal is minor. Noticeably, two broad peaks centred at 316 °C and 485 °C were clearly observed in the profile of Ru/Al–Co catalyst. The former peak can be assigned to the reduction of Co$_3$O$_4$ to CoO and the latter can be attributed to the reduction of CoO to Co.[26]

The acidity analysis of the supported Ru catalysts was carried out by NH$_3$-TPD, and the results were presented in Fig. 5 and Table 2. Two clear peaks were observed in the desorption curves of NH$_3$ for Ru/Al–Mo, Ru/Al–Co and Ru/Al catalysts. The first peak positioned in the range of 200–250 °C is assigned to medium acid sites, and the high-temperature desorption peak positioned in the range of 440–490 °C is assigned to strong acid sites.[27] The acidity of TiO$_2$ is very weak as expected and the amount of acid sites is little.[8] It should be noted that the NH$_3$-TPD profile of Ru/Ti–Al is rather close to that of Ru/Ti catalyst. A possible reason is that TiO$_2$ was coated on the surface of Al$_2$O$_3$,[28,29] leading to the less acidic sites of Ru/Ti–Al catalyst. The type of acidic sites is determined by infrared spectroscopy of pyridine adsorption. It can be found that Lewis acid sites (1450 cm^{-1}) is dominant for all tested catalyst as shown in Fig. 6.

The Ru 3d XPS spectrum of Ru catalyst is presented in Fig. 7. The spectrum in the region of 283–287 eV is complex due to the overlapping of C 1s signal and Ru 3d doublet (5/2 and 3/2).[30] The regions of 281.5–283 eV are assigned to RuO$_x$, suggesting that ruthenium oxides remain at the catalyst surface even after reduction. Normally, the Ru 3d XPS spectrum should show a signal at 280.0 eV, which is attributed to Ru^0.[16] However, the signals of Ru^0 were observed at 280.2 eV for Ru/Al–Mo, 280.4 eV for Ru/Al–Ti and 280.6 eV for Ru/Al–Co, respectively. The small shift of the BE (binding energy) may have been caused by the interaction between the metallic Ru^0 and its support.[31]

Catalyst testing

The hydrogenation of LA to GVL was carried out over the different Ru catalysts in an H$_2$ flow of 40 ml min^{-1} and a WHSV (weight hourly space velocity) of 0.6 h^{-1}. It is clear that the product distribution is significantly affected by catalyst and reaction temperature as shown in Fig. 8. GVL, 2-butanol and 1,4-pentanediol are the major products for the hydrogenation of LA. The lower GVL yield is observed over the Ru/Al–Co and Ru/Al–Mo catalysts in the investigated temperature range while higher GVL yield (80%) is obtained over Ru/Al–Ti catalyst at 80 °C. This difference could be attributed to the acidity of the catalyst. Generally, LA is hydrogenated into 4-hydroxy valeric acid over Ru active sites, and subsequently converted into GVL by dehydration.[8,9] However, intermediate 4-hydroxy valeric acid could be converted to 2-butanol by decarboxylation, and GVL
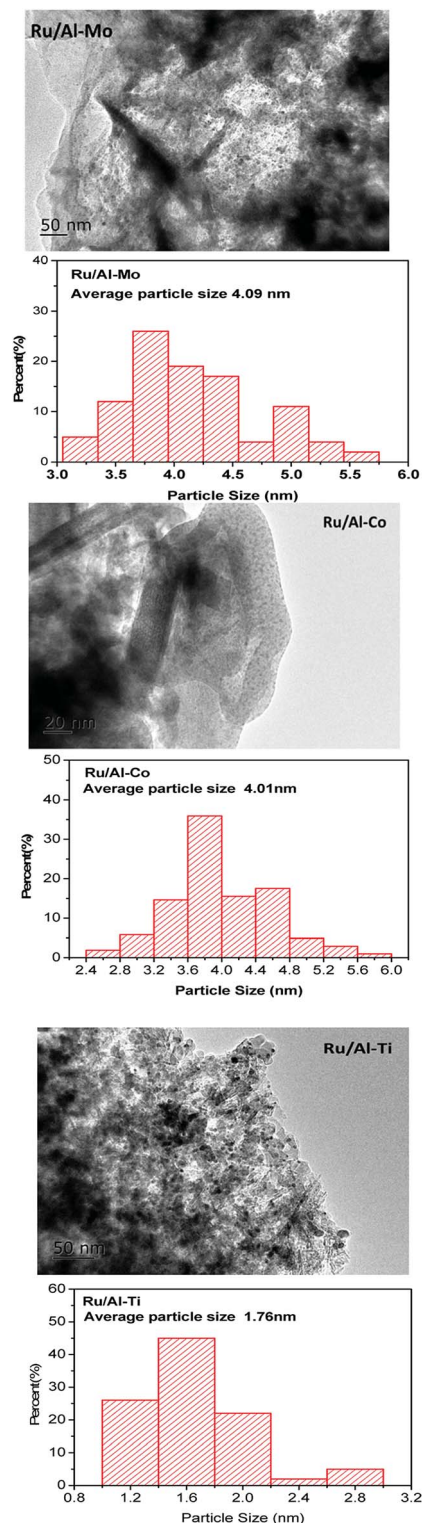
Fig. 3 TEM images of different Ru-based catalysts and their particle size distributions.

Fig. 4 H_2-TPR of the different Ru catalysts.
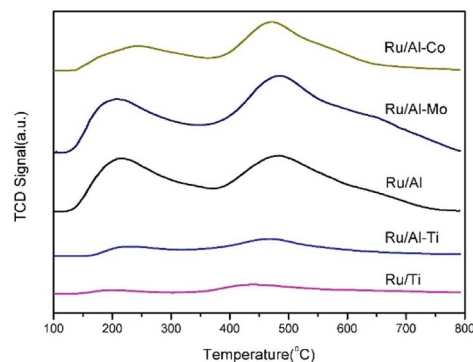
Fig. 5 NH$_3$-TPD profiles of the different Ru catalysts.

could be further converted to 1,4-pentanediol by hydrogenation as shown in Schemes 1. These side reactions are promoted by Ru catalyst with strong acidic support. As discussed in 'NH$_3$-TPD analysis' section, the acidity of Ru/Al–Ti is far less than those of Ru/Al–Co and Ru/Al–Mo. So, it is plausible that the GVL

yield over Ru/Al–Ti catalyst is higher than those of Ru/Al–Co and Ru/Al–Mo catalysts. In addition, side-reactions are favoured at higher temperature. There is a sudden increase of 1,4-pentanediol over Ru/Al–Co and Ru/Al–Mo catalysts at 220 °C. A possible reason is that the conversion of GVL to 1,4-pentanediol was promoted by Ru/Al–Co and Ru/Al–Mo catalysts at higher temperature. As far as Ru/Al–Ti is concerned, the yield of by-product 2-butanol is higher than that of the desired product GVL at 180 °C and 220 °C, as shown in Fig. 8. The major reason is that the decarboxylation reaction of intermediate 4-hydroxy pentanoic acid was promoted at higher temperature, leading to the increase of 2-butanol.

As shown in Fig. 9(a), the components of CO, CO_2, CH_4, C_{2+} were detected in the gas product. These gas products were derived from LA, GVL and intermediates *via* aqueous phase reforming with Ru catalyst. For example, apart from the decarboxylation,[32] the formation of CO_2 may also be considered to be a catalytic decomposition of the reactants to form CO, combined with the conversion of CO and H_2O to produce CO_2. Cleavage of C–C and C–O bonds can be completed by hydrogenolysis over Ru catalyst in the presence of H_2, thereby producing the smaller hydrocarbon molecule.[33] Similar reactions had been reported.[34,35] Arguably, higher temperature can promote the aqueous phase reforming (Fig. 9(b)). This is the reason that LA conversion increases at higher temperature, but the product yield does not increase in synchronization, as shown in Fig. 8.

Table 2 The amounts of acid sites for different Ru catalysts determined by NH_3-TPD

Catalyst	120–345 °C, mmol g^{-1}	345–787 °C, mmol g^{-1}	Total acid sites, mmol g^{-1}
Ru/Al–Mo	0.277	0.291	0.568
Ru/Al–Co	0.124	0.189	0.313
Ru/Al–Ti	0.040	0.063	0.103
Ru/Al	0.279	0.053	0.332
Ru/Ti	0.013	0.042	0.055
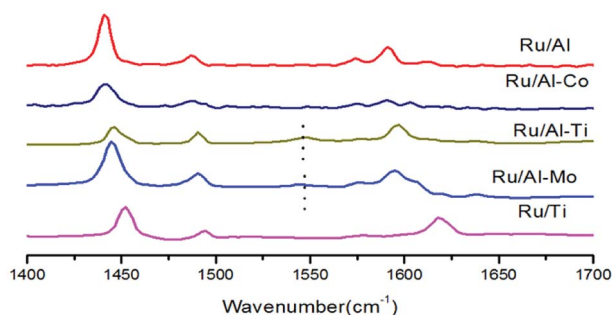
Fig. 6 Infrared spectra of pyridine adsorbed on Ru catalyst after evacuation at 200 °C.

To explore the effect of mixed oxides on the catalytic activity, the hydrogenation of LA over Ru catalyst supported on pure oxide was also conducted at 80 °C. As shown in Fig. 10, the GVL yields were only 41.6% and 21.8% over Ru/Al and Ru/Ti catalysts, respectively. For the Ru/Ti catalyst, the deteriorated porous and small surface area might be the root cause for the lower GVL yield of the Ru/Ti catalyst. As for the Ru/Al catalyst, it is similar to that of Ru/Al–Co and Ru/Al–Mo catalysts, the strong acidity of the catalyst results in the lower yield of desired product. On the contrary, the GVL yield drastically increased to 80% when Ru/Al–Ti was used as catalyst. This result suggests that mixed oxides have significant advantages in improving catalytic activity.

Effect of WHSV

The effect of WHSV was also investigated at 80 °C using Ru/Al–Ti as catalyst. As shown in Fig. 11, GLV yield gradually increased in the range of 0.6–1.8 h^{-1}. It is explained that the product GVL
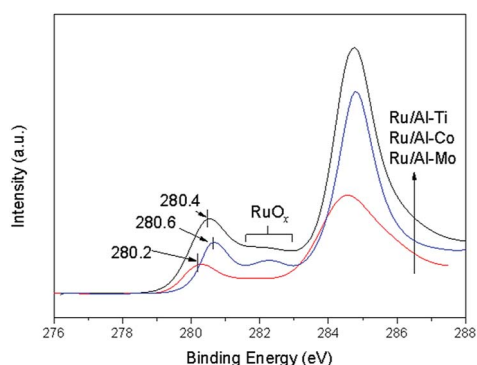
Fig. 7 Ru 3d XPS spectrum of different catalyst.
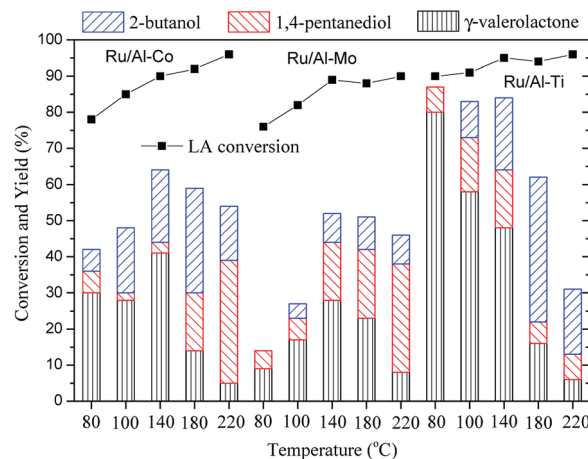
Fig. 8 Conversion of LA to GVL over different Ru catalysts. Reaction conditions. P_{H_2} = 4.0 MPa, H_2 flow: 40 ml min^{-1}; WHSV: 0.6 h^{-1}.

could be taken out instantaneously from the reactor due to the increased WHSV, avoiding the aqueous phase reforming of GVL. However, GVL yield decreased slightly when the WHSV was further increased to 2.4 h^{-1}. Therefore, the next work for conversion of LA to GVL was carried out with a WHSV of 1.8 h^{-1}.

Stability of catalyst

The stability of Ru catalysts was tested with a WHSV of 1.8 h^{-1} at 80 °C. As shown in Fig. 12, GVL yield is about 97% over Ru/Al–Ti catalyst and remains constant within the tested 120 h while the GVL yield is constant at about 26% over Ru/Ti catalyst. As for the Ru/Al catalyst, the GVL yield decreases gradually with the lengthened reaction time. This result suggests that Ru/Al catalyst was deactivated gradually in the reaction process. It had been reported that large amounts of Ru and Al were leached into
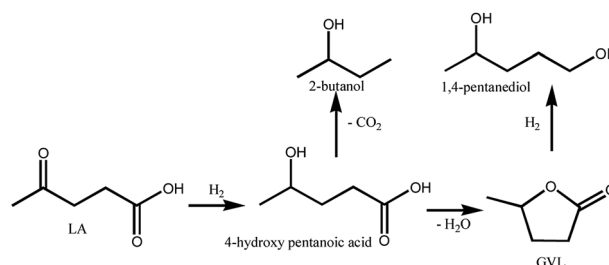
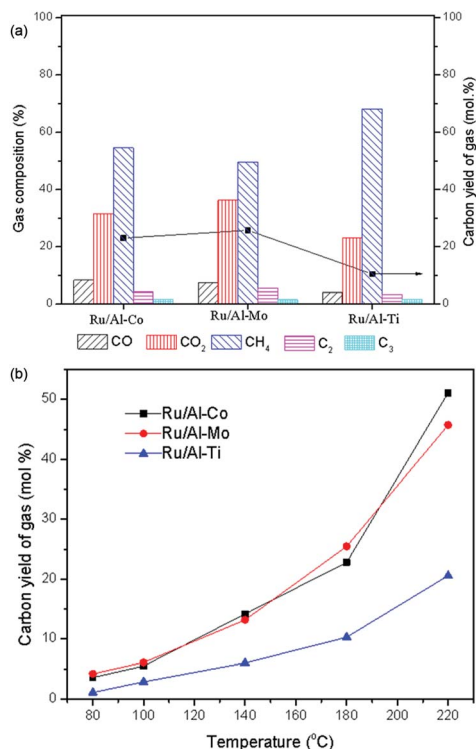**Scheme 1** The possible reaction pathways for conversion of LA to GVL.

Fig. 9 Effects of catalysts and reaction temperature on gas compositions. Reaction conditions: (a) $T = 180\ °C$; $P_{H_2} = 4.0$ MPa, H_2 flow: 40 ml min^{-1}; WHSV = 0.6 h^{-1}; (b) $P_{H_2} = 4.0$ MPa, H_2 flow: 40 ml min^{-1}; WHSV = 0.6 h^{-1}.

the solution during the conversion of LA to GVL with Ru/Al₂O₃ catalyst, which resulted in a decrease in catalytic activity.[18] In this study, we also detected the concentration of aluminium and ruthenium ions in the collected liquid samples, and the results were listed in Table 3. It is clear that the large amount of Al and Ru ions were leached from the Ru/Al catalyst. A reasonable explanation is that the alumina was corroded and leached when exposed to acid (levulinic acid) in the aqueous solution. The interaction between Ru metal and carrier disappears when the γ-Al₂O₃ is leached, resulting in the leaching of Ru. It is thereby plausible that large amount of Al and Ru were detected

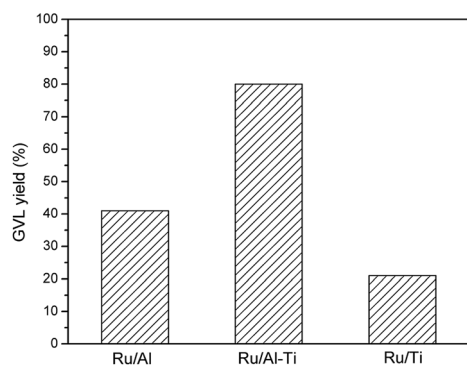Fig. 10 Comparison for the effect of mixed oxides and pure oxide. Reaction conditions: $T = 80\ °C$; $P_{H_2} = 4.0$ MPa; H_2 flow: 40 ml min^{-1}; WHSV = 0.6 h^{-1}.
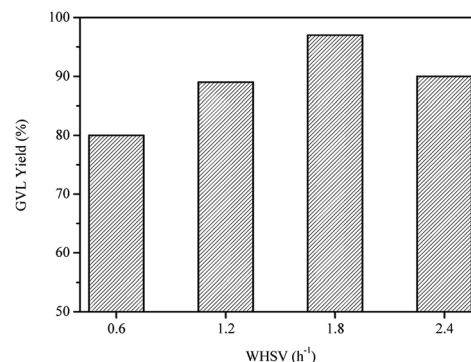

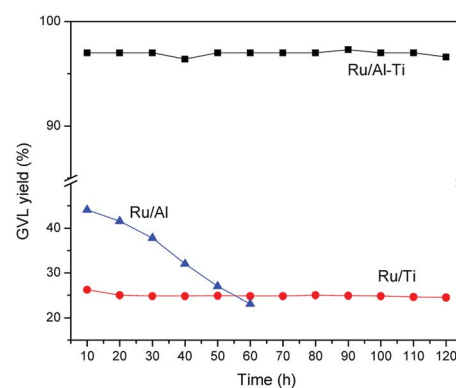Fig. 11 Effect of WHSV on the conversion of LA to GVL over Ru/Al–Ti catalyst. Reaction conditions: $T = 80\ °C$; $P_{H_2} = 4.0$ MPa; H_2 flow: 40 ml min^{-1}.

Fig. 12 The stability test for Ru/Al–Ti catalyst. Reaction conditions: WHSV = 1.8 h^{-1}; $T = 80\ °C$; $P_{H_2} = 4.0$ MPa; H_2 flow: 40 ml min^{-1}.

in the collected liquid sample. Fortunately, leaching of Al and Ru is negligible for Ru/Al–Ti catalyst. This result may strongly suggest that the Ru catalyst supported on Al–Ti mixed oxides possesses excellent stability under hydrothermal condition. The major contribution should be attributed to the added TiO₂ component, which is a kind of acid-tolerant material. It can be inferred that TiO₂ is coated on the surface of Al₂O₃, which prevented the contact between acid and Al₂O₃, reducing the leaching of Al. This inference is consistent with the previous conclusions derived from NH₃-TPD analysis.

Table 3 Aluminium and ruthenium content of liquid samples taken at different runtimes in LA conversion experiments[a]

Catalyst	Time on stream (h)	Total leached Al (wt%)	Total leached Ru (wt%)
Ru/Al	30	2.1	35
	60	3.6	44
Ru/Ti	30	—	0.6
	120	—	0.8
Ru/Al–Ti	30	0.2	1.4
	120	0.4	2.6

[a] Reaction conditions: $T = 80\ °C$; $P_{H_2} = 4.0$ MPa; H_2 flow: 40 ml min^{-1}; WHSV = 1.8 h^{-1}.

Conclusions

Ru catalysts supported on mixed oxides Al_2O_3–TiO_2, Al_2O_3–MoO_3 and Al_2O_3–Co_3O_4 were studied for conversion of levulinic acid to γ-valerolactone. NH_3-TPD results and catalytic behaviour revealed that the Ru metal combined with strong acidic sites of support could promote the aqueous phase reforming, resulting in the lower yield of GVL. TiO_2 might be coated on the surface of Al_2O_3, weakening the acidity of mixed oxides Al_2O_3–TiO_2. Therefore, Ru/Al_2O_3–TiO_2 exhibited better catalytic activity for GVL yield than those of Ru/Al_2O_3–MoO_3 and Ru/Al_2O_3–Co_3O_4. Moreover, Ru/Al_2O_3–TiO_2 exhibited excellent stability under hydrothermal condition.

Conflicts of interest

There are no conflicts to declare.

Acknowledgements

Notes and references

1 S. G. Wettstein, D. M. Alonso, E. I. Gürbüz and J. A. Dumesic, Curr. Opin. Chem. Eng., 2012, 1, 218.
2 J. Zhang and N. Yan, ChemCatChem, 2017, 9, 2790.
3 J. J. Bozell and G. R. Petersen, Green Chem., 2010, 12, 539.
4 I. T. Horvath, H. Medhi, V. Fabos, L. Boda and L. T. Mika, Green Chem., 2008, 10, 238.
5 W. R. H. Wright and R. Palkovits, ChemSusChem, 2012, 5, 1.
6 D. W. Rackemann and W. O. S. Doherty, Biofuels, Bioprod. Biorefin., 2011, 5, 198.
7 J. Tan, Q. Liu, L. Chen, T. Wang, L. Ma and G. Chen, J. Energy Chem., 2017, 26, 115.
8 W. Luo, M. Sankar, A. M. Beale, Q. He, C. J. Kiely, P. C. A. Bruijnincx and B. M. Weckhuysen, Nat. Commun., 2015, 6, 6540.
9 R. Yoshida, D. Sun, Y. Yamada, S. Sato and G. J. Hutchings, Catal. Commun., 2017, 97, 79.
10 X. L. Du, L. He, S. Zhao, Y. M. Li, Y. Cao, H. Y. He and K. N. Fan, Angew. Chem., Int. Ed., 2011, 50, 7815.
11 P. P. Pravin, J. M. Lee, D. W. Hwang, S. B. Halligudi, Y. K. Hwang and J. S. Chang, J. Ind. Eng. Chem., 2011, 17, 287.
12 A. M. Hengne and C. V. Rode, Green Chem., 2012, 14, 1064.
13 D. J. Braden, C. A. Henao, J. Heltzel, C. C. Maravelias and J. A. Dumesic, Green Chem., 2011, 13, 1755.
14 W. Deng, Y. Wang, S. Zhang, K. M. Gupta, M. J. Hülsey, H. Asakura, L. Liu, Y. Han, E. M. Karp, G. T. Beckham, P. J. Dyson, J. Jiang, T. Tanaka, Y. Wang and N. Yan, Proc. Natl. Acad. Sci. U. S. A., 2018, 115, 5093.
15 Y. Wang, S. De and N. Yan, Chem. Commun., 2016, 52, 6210.
16 R. S. Suppino, R. Landers and A. J. G. Cobo, Appl. Catal., A, 2016, 525, 41.
17 C. Moreno-Marrodan and P. Barbaro, Green Chem., 2014, 16, 3434.
18 A. S. Piskun, J. E. de Haan, E. Wilbers, H. H. van de Bovenkamp, Z. Tang and H. J. Heeres, ACS Sustainable Chem. Eng., 2016, 4, 2939.
19 M. Sudhakar, M. Lakshmi Kantam, V. Swarna Jaya, R. Kishore, K. V. Ramanujachary and A. Venugopal, Catal. Commun., 2014, 50, 101.
20 A. S. Amarasekara and M. A. Hasan, Catal. Commun., 2015, 60, 5.
21 P. P. Upare, J. M. Lee, Y. K. Hwang, D. W. Hwang, J. H. Lee, S. B. Halligudi, J. S. Hwang and J. S. Chang, ChemSusChem, 2011, 4, 1749.
22 M. Chia and J. A. Dumesic, Chem. Commun., 2011, 47, 12233.
23 G. Murali Dhar, B. N. Srinivas, M. S. Rana, M. Kumar and S. K. Maity, Catal. Today, 2003, 86, 45.
24 A. Primo, P. Concepcion and A. Corma, Chem. Commun., 2011, 47, 3613.
25 X. Zhang, T. Wang, L. Ma and C. Wu, Fuel, 2010, 89, 2697.
26 T. M. Sankaranarayanan, A. Berenguer, C. Ochoa-Hernández, I. Moreno, P. Jana, J. M. Coronado, D. P. Serrano and P. Pizarro, Catal. Today, 2015, 243, 163.
27 S. Pichaikaran and P. Arumugam, Green Chem., 2016, 18, 2888.
28 V. Rodríguez-González, R. Zanella, G. Angel and R. Gómez, J. Mol. Catal. A: Chem., 2008, 281, 93.
29 A. Adamczyk and E. Długoń, Spectrochim. Acta, Part A, 2012, 89, 11.
30 J. Balcerzak, W. Redzynia and J. Tyczkowski, Appl. Surf. Sci., 2017, 426, 852.
31 P. P. Upare, M. Lee, S.-K. Lee, J. W. Yoon, J. Bae, D. W. Hwang, U.-H. Lee, J.-S. Chang and Y. K. Hwang, Catal. Today, 2016, 265, 174.
32 L. Chen, Y. Li, X. Zhang, Q. Zhang, T. Wang and L. Ma, Appl. Catal., A, 2014, 478, 117.
33 G. W. Huber and J. A. Dumesic, Catal. Today, 2006, 111, 119.
34 G. W. Huber, R. D. Cortright and J. A. Dumesic, Angew. Chem., Int. Ed., 2004, 43, 1549.
35 J. N. Chheda, G. W. Huber and J. A. Dumesic, Angew. Chem., Int. Ed., 2007, 46, 7164.